

III. DISLOCATION MOBILITY AND GENERATION

Dislocation Motion and Plastic Yield of Crystals

BY P. HAASEN

Institut für Metallphysik, Universität Göttingen, Hospitalstrasse 12,
Göttingen, Germany

Received 11th June, 1964

A brief summary is presented of the micromechanical approach to crystal plasticity which attempts to calculate plastic properties from direct measurements of dislocation density and dislocation velocity. This approach has been particularly successful in the diamond cubic structure in which dislocations move viscously, interact by their long-range elastic stresses, and multiply exponentially with time under an applied stress. It is shown that an equation of state holds from which the dynamic yield point as well as the initial creep behaviour can be calculated.

It is generally accepted that under normal conditions plastic deformation of crystals occurs by the movement of individual dislocations. A dislocation is a one-dimensional lattice defect which moves on certain crystallographic planes. By its movement it displaces the crystal above relative to that below the slip plane by the Burgers vector b (of a length of about 10^{-8} cm). Some crystals can be deformed to plastic shear strains of 100 % in a period of minutes under shear stresses of the order of magnitude 1 kg mm^{-2} . That means that many dislocations must participate which move easily and quickly. There is a simple kinematical relation¹ (for straight dislocations) between the plastic shear strain rate $\dot{\epsilon}_{P1}$, the total length per cm^3 N of moving dislocations, and the average dislocation velocity v

$$\dot{\epsilon}_{P1} = Nbv. \quad (1)$$

The micro-mechanical approach to crystal plasticity which will be described in the following, attempts to calculate $\dot{\epsilon}_{P1}$ from independent measurements of N and of v as a function of stress and strain according to eqn. (1). These measurements are now possible by methods, first applied by Gilman and Johnston² to LiF, of direct observation which give the velocity of individual dislocations as well as their density. The density N depends on strain due to the process of dislocation multiplication and annihilation and on stress because of the (elastic) interaction between the lattice distortions around dislocations. The latter effect also diminishes the velocity of dislocations under a given applied stress.

Two types of experiments are being used to establish the macroscopic plastic properties of a crystal. In the *dynamic* test the strain rate is kept constant and the work hardening curve $\tau = \tau(\epsilon, \dot{\epsilon})$ is determined. In the *static* or creep test the applied stress τ is constant and the creep curve $\dot{\epsilon} = \dot{\epsilon}(\epsilon, \tau)$ is recorded. Both give the same information if an equation of state is valid (at not too high temperatures). The dynamic test is complicated by an elastic shear strain rate $\dot{\epsilon}/G$ (G = shear modulus) which is to be added to $\dot{\epsilon}_{P1}$ in eqn. (1). The combination of both terms gives rise to the yield phenomenon which is a major subject of this paper.

Although these considerations apply to all types of crystalline materials, we will discuss mainly the diamond structure as an example. Crystals like germanium,

silicon (and InSb with the related sphalerite structure) have some definite advantages in the measurement of v and N and in the calculation, from these dislocation parameters, of the initial stages of work-hardening and creep curves. Firstly, they are available as semiconductor materials in a state of high chemical and structural perfection. Secondly, due to the covalent bond these crystals are brittle at low temperatures and become ductile only gradually at elevated temperatures. This is related to the fact that dislocations in Ge and Si move in a viscous manner, the velocity depending exponentially on temperature T and (almost) linearly on τ . The former parameter, temperature, is, however, much easier to control experimentally than the latter, (stress), which is subject to local fluctuations. Just the opposite situation prevails in ductile metals of f.c.c. and c.p.h. structure and also in salts with the NaCl structure which show a large stress dependence and small temperature dependence of v . This makes a similar study of these crystals rather difficult. B.c.c. metals and solid solution alloys appear to be intermediate with respect to the T and τ dependence of v . In the following, measurements of N and v for Ge and Si are described and interpreted theoretically. The results of these are applied to a calculation of the dynamic and static yield behaviour of these crystals.

DIRECT OBSERVATION OF DISLOCATION MULTIPLICATION

A number of methods have now been developed to "see" dislocations in a crystal. These methods are being discussed at this meeting. Germanium and silicon are rather favourable substances for a direct observation of dislocations. *As-grown crystals* of these semiconductor materials generally contain a dislocation density N_0 smaller than 10^4 cm/cm³, while in metals initial dislocation densities normally are found to be above 10^6 cm/cm³ (N_0 can, however, be lowered to 10^3 cm/cm³ in these crystals by annealing). Within the first percent of deformation the dislocation density increases to about 10^8 cm/cm³. In this range of plastic yield, etch pit methods are particularly suitable for studying dislocations. In the following, results of Alexander and Schröter³ on Ge will be described briefly to illustrate dislocation multiplication in the beginning of a dynamic compression test. The stress-strain curve in this case begins with a pronounced but smooth yield-point as shown in fig. 1. New dislocations appear when the stress reaches a value of about $0.6 \tau_{uy}$. For a low grown-in density ($N_0 < 5000$ cm/cm³) these dislocations move into the specimen from the ends in the form of Lüders band while the stress passes through the upper yield point. In this case, the dislocation distribution as well as the local strain and local strain rate are very inhomogeneous over the length of the specimen even when the stress reaches the lower yield point (τ_{ly}). For larger N_0 these inhomogeneities are less pronounced and a nearly homogeneous distribution is reached at τ_{ly} , as shown in fig. 2. The authors observe that dislocation multiplication ceases in any particular region of the crystal when a density $N(\tau)$ is reached which is related to the stress under which this region deforms. When the limiting density is reached, dislocation motion stops in this part of the crystal and it does not further contribute to $\dot{\epsilon}$. The limiting dislocation density N is related to the instantaneous value of the stress τ by

$$\tau = AN^{\frac{1}{2}} \quad (2)$$

In a calculation of the total strain rate of the specimen at any stress from N (and v , see below) according to eqn. (1) one has to leave out all the "dead" areas with $\tau \leq AN^{\frac{1}{2}}$. Eqn. (2) theoretically describes the mean internal stress of a statistical distribution of positive and negative dislocations, according to Taylor, with $A = \alpha Gb$. Theoretically, $\alpha = 1/2\pi(1-\nu)$, ν = Poisson's ratio; i.e., $\alpha \approx 0.25$, for edge dislocations,

while experimentally $\alpha \approx 0.3$ for germanium. Thus, dislocation multiplication stops when the mean internal stress of the dislocations created balances the applied stress.

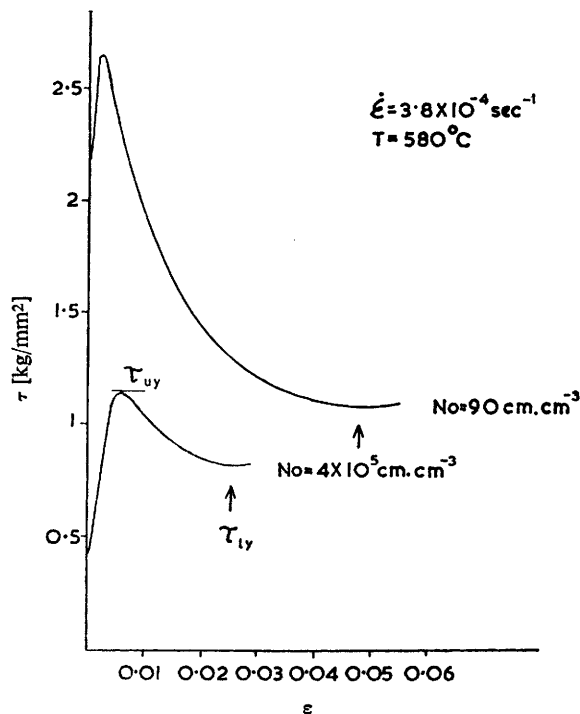


FIG. 1.—Shear stress-shear strain curves of two germanium single crystals with different grown-in dislocation densities N_0 , from ref. (3).

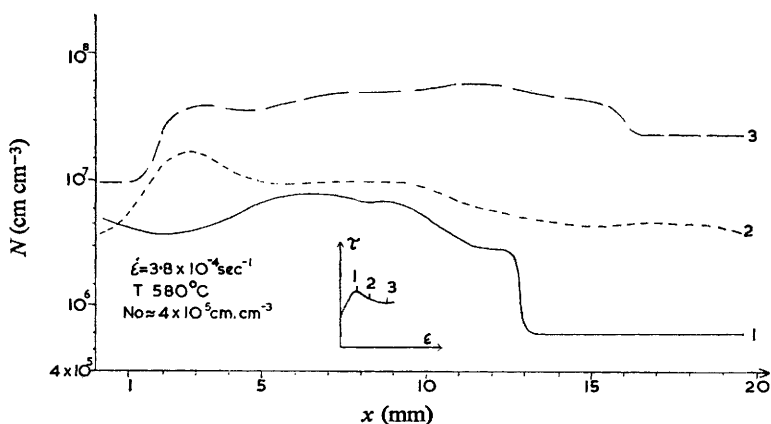


FIG. 2.—Dislocation density along a Ge compression specimen at various points (1, 2, 3) of the stress strain curve, as indicated.³

We do not know in detail from these etch pit observations how dislocations multiply. It follows from the study of the deformation inhomogeneity mentioned above and from the general N_0 -dependence of the yield phenomenon (see below) that grown-in dislocations must assist in activating sources if they do not multiply

themselves. The effect of varying specimen dimensions on the creep of InSb indicates that surface sources are not important.⁴ From electron transmission pictures of germanium slices cut from deformed crystals, Alexander⁵ concludes that edge dislocation dipoles formed at long jogs in screws constitute potential sources for dislocation multiplication. The partners of a dipole may pass by each other when the stress increases and develop into a dislocation loop as indicated in fig. 3. The mechanism by which a large jog is formed is still uncertain; it probably gains in height as the

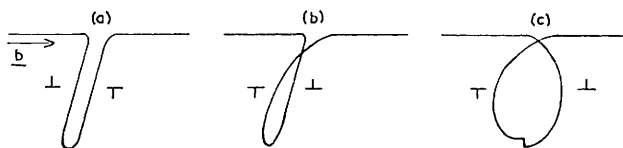


FIG. 3.—(a)–(c): crossing-over of a dislocation dipole forming a new dislocation loop.

original screw moves along. This will lead to an *exponential* dislocation multiplication according to the relation

$$dN = \delta N v dt, \quad (3)$$

where the multiplication constant δ , determined by the process of two edge dislocations being able to pass each other, is proportional to stress. A similar multiplication law has been proposed by Gilman² for the double-cross slip mechanism in LiF, while Low and Turkalo⁶ in Fe + 3.0% Si observed the “crossing-over” mechanism described above.*

Actually, the letter N , dislocation density, in eqn. (1)–(3), is used in two different meanings. While the dislocations entering eqn. (1) and (3) must clearly be mobile ones, N in eqn. (2) counts all the dislocations left in the crystal after a strain increment whether they are mobile or immobile. However, most of the dislocations get stuck as edge dipoles, which do not have long-range stresses contributing to τ in eqn. (2). This may be the reason why the simplification of using the same N in eqn. (1)–(3) works well for small deformations. At large ϵ (stages I–III of the stress-strain curve) the approximation fails because, among other things, dislocations which do exert long-range stresses get stuck in the crystal.

MEASUREMENT AND INTERPRETATION OF DISLOCATION VELOCITIES

Gilman and Johnston² first measured dislocation velocities by a double etching technique. The dislocation positions in a region of a crystal are first determined by etching. Then the crystal is loaded to a stress τ for a time Δt and re-etched. Dislocations are found by the new etch to have moved an average distance Δx (see fig. 4). Making sure that Δx is proportional to Δt , one defines $v = \Delta x / \Delta t$. The velocity has thus been determined as a function of stress τ and temperature T for various substances, particularly for Ge, Si, InSb.^{2, 8, 9, 10} The results (except for low temperatures where the situation is more complicated⁹), are best described empirically by the relation,

$$v = B_0(\tau/\tau_0)^m \exp(-U/kT), \quad \tau_0 = 1 \text{ kg/mm}^2, \quad (4)$$

where $m \sim 1.5$ for the diamond structure⁸ ($m \sim 16$ for LiF²; such high m values actually imply an exponential τ dependence). Thus, in Si, Ge, and InSb dislocations

* Dislocation multiplication by a fixed number of Frank-Read sources⁷ (length l_0 , spatial density M) instead of eqn. (3) leads to $dN = M(v^2/l_0)l_0 dt$, which does not fit the experimental data on diamond-structure crystals.

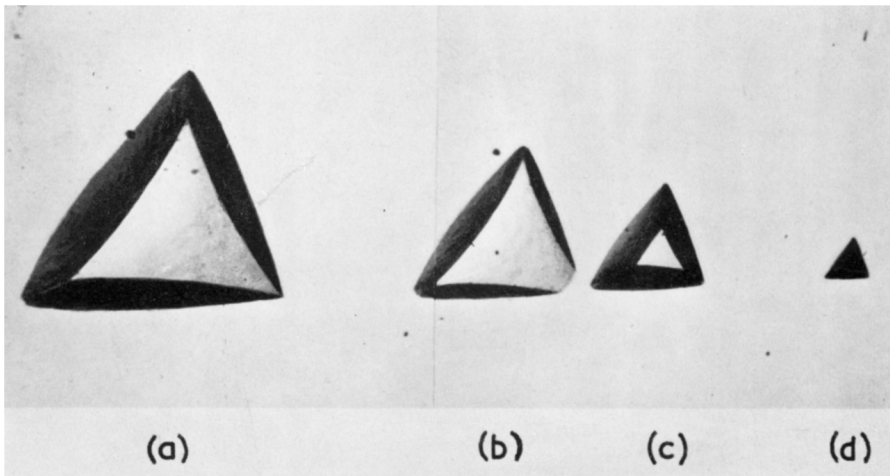


FIG. 4.—Multiple etching of the site of a dislocation which moves from (a) to (b), (c), (d) while the Ge crystal is loaded to 0.5 kg/mm^2 three times for 3 min at 460°C (according to Schäfer¹⁰).

[To face page 194.

move in a viscous manner, the activation energies being ⁸ $U = 1.6$ eV for Ge, $U = 2.2$ eV for Si, $U = 0.7$ eV for InSb.

The theoretical interpretation of eqn. (4) for the diamond structure has been the subject of intense speculation recently.¹¹⁻¹⁵ It is clear that these covalent crystals have a relatively high Peierls energy barrier¹⁴⁻¹⁶ and that kink nucleation and/or kink migration might be the process underlying eqn. (4) and determining the movement of a dislocation. Labusch¹⁵ recently calculated the Peierls barrier of germanium in a model¹ treating forces across the slip plane by a short-range atomotentiipcal fitted to the elastic constants, to the lattice vibration spectrum, and to the energy of dissociation. Outside the slip plane the continuum approach is used. The Peierls energy comes out to be ~ 0.5 eV for a 60° dislocation in Ge. For the energy to form a double kink, to be identified with U , Labusch obtains ~ 1.5 eV. Suzuki¹⁴ in a rather cruder calculation obtains values closer to experiment: $U = 1.67$ eV for Ge, $U = 2.3$ eV for Si. These activation energies correspond to about half the activation energy of self-diffusion and are slightly decreased by the stress according to theory¹⁵ and experiment.⁸ According to Holt¹² the stress dependence of v in eqn. (4) probably stems from kink migration along the dislocation. Celli *et al.*¹³ discuss dislocation motion under the assumption that the migrating kink has to overcome various "dragging points", as proposed earlier by van Bueren.⁷ The process of kink migration along a dislocation is, however, not yet clear. Qualitatively, a linear stress dependence of v is expected from the cracked core model of a 60° -dislocation in the diamond structure according to Haasen.¹¹

CONSTRUCTION OF THE STRESS STRAIN CURVE FROM EQN. (1)

Using the micro-mechanical data described, one can now calculate from eqn. (1) the beginning of the stress-strain curve obtained in a dynamical experiment. Johnston¹⁷ in a similar calculation for LiF assumes an empirical work-hardening rate to decrease the applied stress as strain progresses. We take into account the (partial) compensation of the applied stress by an internal stress according to eqn. (2).¹⁸ This means that v and δ in eqn. (3) and (4) are determined by an *effective* stress $(\tau - AN^{\frac{1}{2}})$, i.e., $\delta = K(\tau - AN^{\frac{1}{2}})$, $v \propto (\tau - AN^{\frac{1}{2}})^m$. Then eqn. (1) turns into the following set of differential equations for $\tau(N(t))$ ¹⁹ (with $B = B_0\tau_0^m \exp(-U/kT)$):

$$\begin{aligned} \dot{\epsilon} &= \dot{\epsilon}_{pl} + \dot{\epsilon}_{el} = bBN(\tau - AN^{\frac{1}{2}})^m + \dot{\tau}/G, \\ \dot{N} &= KBN(\tau - AN^{\frac{1}{2}})^{m+1}. \end{aligned} \quad (5)$$

These equations have been solved numerically²⁰ for various N_0 , neglecting yield propagation effects. The qualitative features of the stress-strain curve following as a solution of eqn. (5) and the T - and $\dot{\epsilon}$ -dependence of its characteristic parameters can, however, be easily evaluated.

The strain rate $\dot{\epsilon}$ applied to the crystal is first carried elastically by a rise of τ (according to the $\dot{\epsilon}_{el}$ term in eqn. (5)). At a finite stress, the (relatively small) initial dislocation density N_0 starts to multiply and a plastic contribution to strain rate results. The elastic term, i.e., the rise of τ with time, can then decrease, become zero and even negative as the plastic term increases. The stress thus goes through an upper yield point. It would fall to zero were it not for work-hardening according to eqn. (2) which limits dislocation multiplication and lets the stress rise again. A (lower) yield point therefore is explained as shown in fig. 1 (for two N_0 values). In agreement with this model, the upper yield stress decreases with increasing N_0 and disappears for large N_0 (of the order of $N(\tau_{ly}) = \left(\frac{2}{m+2} \frac{\tau_{ly}}{A}\right)^2 \sim 10^7 \text{ cm}^{-2}$).^{3, 21}

A high-temperature anneal of such a specimen restores the pronounced yield point as

it decreases N to a value below $N(\tau_{ly})$.²² The theory¹⁹ expects the lower yield stress to be *independent* of N_0 . Experimentally τ_{ly} shows a smaller N_0 dependence than τ_{uy} , but still τ_{ly} is larger for a small N_0 .^{3, 22} It is evident, however, that any strain

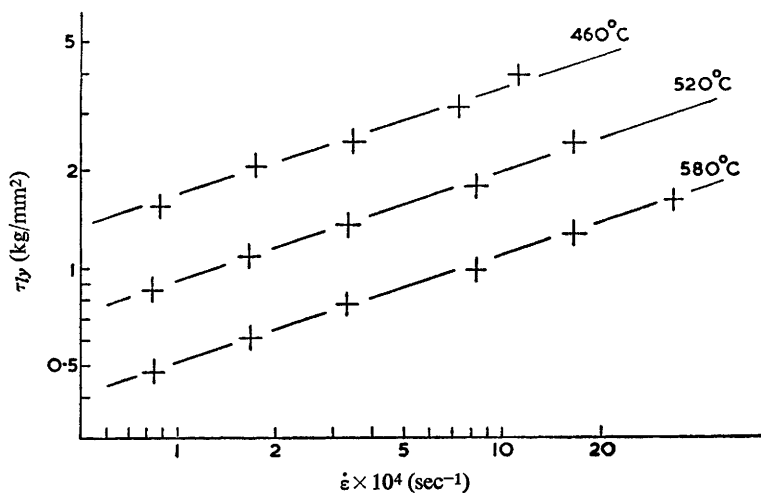


FIG. 5.—Strain-rate dependence of the lower yield stress of Germanium.²³

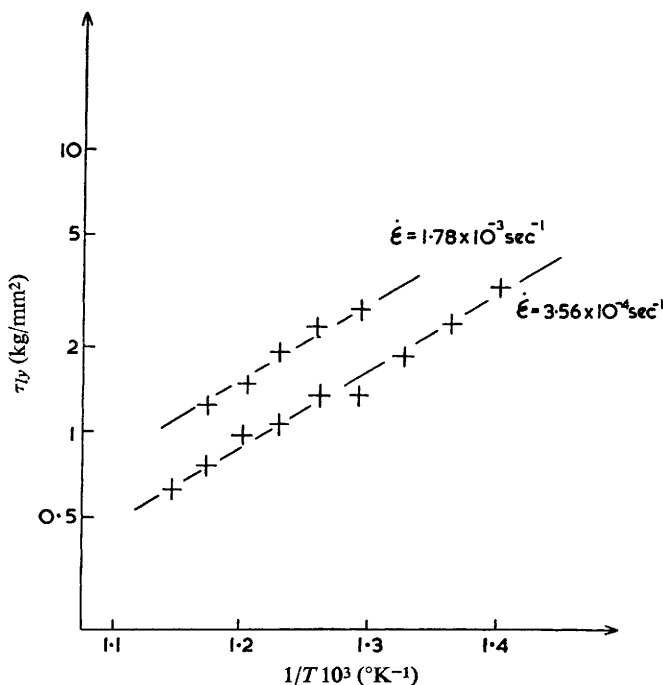


FIG. 6.—Temperature dependence of the lower yield stress of Germanium.²³

inhomogeneity of the kind discussed above will increase the effective strain rate and therefore τ_{ly} for small N_0 . This effect makes a realistic calculation of τ_{uy} rather difficult²⁰ as deformation at the upper yield point is always inhomogeneous. At

the lower yield stress, the homogeneous theory applies for not too small N_0 . Here the elastic term in eqn. (5) can be neglected. This easily leads to,^{4, 18, 19}

$$\tau_{ly} = \tau_0 (A^2 C_m / b B_0)^{1/(2+m)} \dot{\epsilon}^{1/(2+m)} \exp(U/(2+m)kT), \quad (6)$$

where $C_m = \left(1 + \frac{2}{m}\right)^{m+2} \left(\frac{m}{2}\right)^2 = 6.75$ for $m = 1$. In eqn. (6) all parameters are known from direct micro-mechanical measurements. It can be checked by a macroscopic investigation²³ of $\tau_{ly}(\dot{\epsilon}, T)$. The results for Ge are shown in fig. 5 and 6 and are best described by eqn. (6) with $m = 1.1$, $U = 1.64$ eV, $A = 6.2 \times 10^{-3}$ kg cm⁻¹, i.e., $\alpha \sim 0.3$, in good agreement with the data obtained above. For InSb similar experiments²³ give a rather larger $U = 0.96$ eV than direct v -measurements. The m -values of macroscopic experiments are always closer to one than the micro-mechanical results. For relatively large N_0 the upper yield stress shows a similar T and $\dot{\epsilon}$ dependence as τ_{ly} according to both theory¹⁹ and experiment.²³ The dependence of stress on strain in a region following the yield point ("stage 0") also is well described by our theory.¹⁹

CALCULATION OF THE CREEP CURVE FROM EQN. (1)

The pronounced yield-point in a dynamic experiment corresponds to an S-shaped initial creep curve under constant stress as drawn in fig. 7b. While at τ_{ly} stress is constant at a prescribed $\dot{\epsilon}$, in the static test there is steady state creep, $\dot{\epsilon} = \dot{\epsilon}_w$ under a given τ . The constant creep rate $\dot{\epsilon}_w$ follows by simple inversion of eqn. (6):

$$\dot{\epsilon}_w = \frac{b B_m \tau_0^2 \left(\frac{\tau}{\tau_0}\right)^{m+2}}{A^2 C_m} \exp\left(\frac{-U}{kT}\right). \quad (7)$$

Fig. 7a shows the calculated variation of N , v and $\dot{\epsilon}_P$ along the creep curve according to eqn. (1) and (5). (The elastic strain is a constant in this case.) The creep strain at first increases exponentially with time. The curve is characterized by an incubation time t_w and a strain ϵ_w at the inflexion point (as well as by $\dot{\epsilon}_w$). Integration of eqn. (5) again has been done numerically,⁴ but the following approximate expressions are easily obtained.¹⁹

$$t_w = f/(KB_0 \tau_0)(\tau_0/\tau)^{m+1} \exp(U/kT), \quad (8)$$

$$\epsilon_w = \frac{b\tau}{KA^2} D_m, \text{ with } D_m = 2 \ln\left(\frac{m+2}{m}\right) - \frac{4}{m+2}. \quad (9)$$

For $N_0 > 0$, $m \approx 1$, the factor f in eqn. (8) is approximated by $f = (2.7 + \ln(\tau/AN_0^{\frac{1}{2}}))$. It is clear from eqn. (7) to (9) that the ratio $(\dot{\epsilon}_w t_w / \epsilon_w)$ should be independent of T and nearly of τ , which is borne out by experiments discussed below. Also eqn. (7) and the corresponding eqn. (6) are independent of the particular mechanism of dislocation multiplication as expressed by eqn. (3): $\dot{\epsilon}_w$ and τ_{ly} follow only from eqn. (1) and (2).

The theory has been applied to creep experiments on InSb,⁴ Ge²⁴ and Si.²⁵ Those on InSb have been performed in three-point-bending and had to be corrected for absolute ϵ and τ -values by concurrent bending and compression experiments on Ge.²⁴ The results are generally in good numerical agreement with theory, the parameters of which can be compared with micromechanical data. (For InSb, creep tests⁴ give $U = 0.88$ eV, $m \sim 1.5$, $\delta \sim 200$ cm⁻¹, $\alpha \sim 0.5$; for Ge²⁴ $U = 1.75$ eV, $m \sim 1.2$).

Of particular interest are compression creep data²⁵ obtained with silicon single crystals of two different grown-in dislocation densities $N_{02} = 2 \times 10^4$ cm⁻², $N_{01} = 0$. Typical creep curves of N_{01} -crystals fitted to the calculated curve at the inflexion point are shown in fig. 8. The co-ordinates of this point are plotted according to eqn. (7)

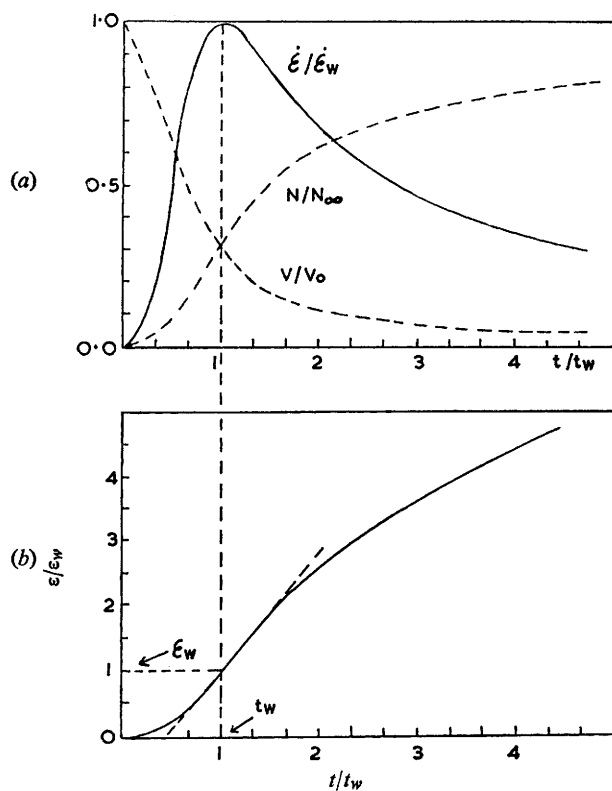


FIG. 7.—Creep curve (b), calculated from dislocation density N and dislocation velocity v (a) according to eqn. (1).⁴

FIG. 8.—Comparison of measured creep curves of silicon²⁵ with calculated curve⁴ (solid line) ($T = 900^\circ\text{C}$, $\tau(\text{kg mm}^{-2}) = 0.2$, +; 0.3 , \square ; 0.4 , \circ ; 0.7 , \times ; $\tau = 0.5 \text{ kg mm}^{-2}$, $T(^{\circ}\text{C}) = 940$, \blacktriangledown ; 881 , ∇ ; 856 , \bullet ; 803 , \blacksquare).

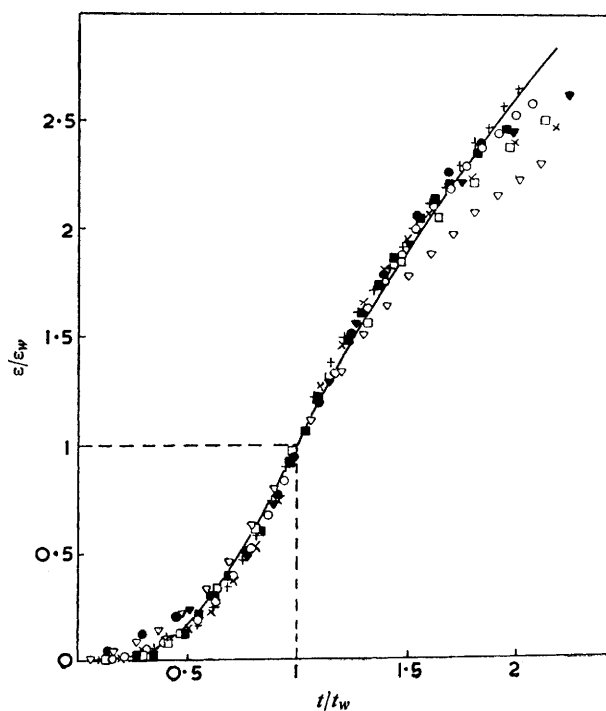


FIG. 9.—Temperature dependence of creep parameters of silicon²⁵ (●, dislocation-free crystal).

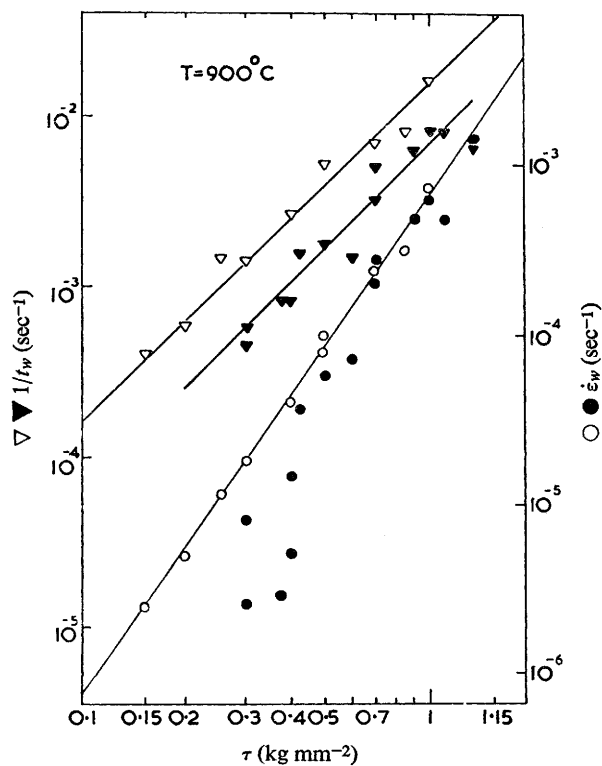
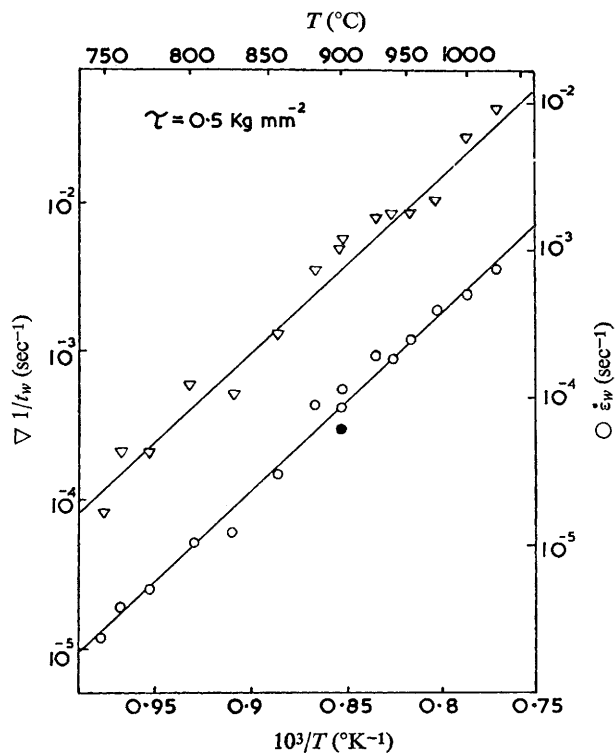


FIG. 10.—Stress dependence of creep parameters of silicon²⁵ (●, ▼ mark initially dislocation-free crystals, $N_{02} = 0$; ○, ▽ crystals with $N_{01} = 2 \times 10^4 \text{ cm}^{-2}$).

and (8) in fig. 9 and 10. From the slopes one obtains $m = 1 \pm 0.01$, $U = 2.4 \pm 0.05$ eV for silicon. Furthermore, $\epsilon_w/\tau = \text{const.} = 2 \text{ \%}/\text{kg}/\text{mm}^{-2}$ in agreement with eqn. (9) and dynamical data (on ϵ_{ly}/τ_{ly}).²³ Data points for dislocation free crystals are also shown in fig. 9 and 10. While $\dot{\epsilon}_w$ is independent of N_0 for large τ as required by (homogeneous slip) theory, it decreases at small τ relative to N_{01} crystals. As expected, the incubation time of the N_{02} specimen is much larger than that of N_{01} specimen over the whole stress range. (For $\tau < 0.25 \text{ kg}/\text{mm}^2$ no creep was observed at all at 900°C over 3 h). $N_0 = 0$ is a singular case, and dislocations are probably created on the faces in contact with the compression plates. The general features of the theory on the N_0 -dependence of the initial creep period are, however, clearly observed.

In conclusion, it might be stated that the plastic yield of crystals with the diamond structure can be successfully resolved into a few simple dislocation processes which are themselves accessible to direct measurement. Germanium, and particularly silicon, appear to be ideal materials for plasticity studies as dislocations move in them under an applied shear stress with a *Newtonian viscosity*. We have no doubt that the method also can explain the yield behaviour of other materials of high perfection and strong friction against dislocation motion.

The author is grateful for the continued co-operation of Dr. Helmut Alexander and a group of research students on whose work this report is based. Dr. M. F. Ashby kindly commented on the manuscript. This work has been supported by the Deutsche Forschungsgemeinschaft.

¹ Cottrell, *Dislocations and Plastic Flow in Crystals* (Clarendon Press, Oxford, 1953).

² Gilman and Johnston, in *Solid State Physics*, ed. F. Seitz and D. Turnbull (Academic Press, New York, 1962, **13**, 147.

³ Alexander, Haasen and Schröter, *Phys. Stat. Sol.*, 1964, **7**, 983, cf. Schröter, *Dipl. Thesis* (Göttingen, 1964).

⁴ Peissker, Haasen and Alexander, *Phil. Mag.*, 1961, **7**, 1279.

⁵ Alexander, H., private communication.

⁶ Low and Turkalo, *Acta Met.*, 1962, **10**, 215.

⁷ van Bueren, *Physica*, 1959, **25**, 775; 1960, **26**, 997.

⁸ Chaudhuri, Patel and Rubin, *J. Appl. Physics*, 1962, **33**, 2736; 1963, **34**, 240.

⁹ Kabler, *Physic. Rev.*, 1963, **131**, 54.

¹⁰ Schäfer, S., unpublished results, Göttingen, 1964.

¹¹ Haasen, *Acta Met.*, 1957, **5**, 598.

¹² Holt and Dangor, *Phil. Mag.*, 1963, **8**, 1921.

¹³ Celli, Kabler, Ninomiya and Thomson, *Physic. Rev.*, 1963, **131**, 58.

¹⁴ Suzuki, *J. Physic. Soc. Japan*, 1963, **18**, suppl. I, 182.

¹⁵ Labusch, *Phys. Stat. Sol.*, to be published.

¹⁶ Celli, *J. Physics Chem. Solids*, 1961, **19**, 100.

¹⁷ Johnston, *J. Appl. Physics*, 1962, **33**, 2716.

¹⁸ Haasen, *Z. Physik*, 1962, **167**, 461.

¹⁹ Haasen, in *Festkörperprobleme*, ed. Sauter (Vieweg, Braunschweig, 1965), vol. III, p. 167.

²⁰ Alexander, H., to be published.

²¹ Patel and Chaudhuri, *J. Appl. Physics*, 1963, **34**, 2788.

²² Bell and Bonfield, *Phil. Mag.*, 1964, **9**, 9.

²³ Schäfer, Alexander and Haasen, *Phys. Stat. Sol.*, 1964, **5**, 247.

²⁴ Alexander, H. and Hewing, J., to be published, cf. Hewing, J., *Dipl. Thesis* (Göttingen, 1963).

²⁵ Reppich, Haasen and Ilschner, *Acta Met.*, 1964, **12**, 1283; cf. Reppich, B., *Dipl. Thesis* (Göttingen, 1963).